MICROSTRUCTURE EVOLUTION IN PLASTIC DEFORMATION OF ZIRCONIUM BY COMPRESSION

A. PÖTZSCH* AND P. KLIMANEK

Freiberg University of Mining and Technology, Institute of Physical Metallurgy,
D-09596 Freiberg/Sa., Germany

ABSTRACT

Using a commercial testing system MTS 810 flow curves of polycrystalline zirconium with a mean grain size of 11µm were measured in compression tests at RT ($T/T_m = 0.14$) and the interrelations between the deformation conditions and the microstructure evolution of the material were studied by means of light microscopy, X - ray diffractometry (peak -broadening and texture analysis), and in some cases also by SEM (EBSP - technique). The results indicate strong interrelations between mechanical twinning and dislocation slip, which give rise to significant texture changes and an unexpected strain - dependence of the X - ray diffraction peak broadening. Due to multiple twinning three regions of texture development characterised by different volume fractions of the texture components {10.0}, {11.0} and {00.1} are observed.

The dependence of the line broadening of the X-ray lines of the crystallites of the observed texture components {10.0}, {11.0} and {00.1} from the strain ε is very similar to the texture development in the material. The defect content of crystallites belonging to the various texture components is considerable different.

KEYWORDS

Zirconium, compression test, X-ray diffractometry, EBSP- technique, texture analysis, peak – broadening analysis, mechanical twinning, dislocation slip, dislocation density.

INTRODUCTION

Although the technical importance of hexagonal metals and alloys is continuously increasing, their deformation behaviour is less well investigated than that of cubic materials and improved quantitative knowledge of structure - process and/or structure - property interrelations occurring in various modes of plastic deformation is required. In the present study the microstructure evolution in polycrystalline zirconium during compression tests at RT is characterised. Following the methodology of former investigations on compressed magnesium [1,2] and titanium [3,4], particularly the X - ray powder diffractometry (peak – broadening and texture analysis) is used for this purpose and it can be shown, that it is an efficient tool for the determination of physically realistic substructure parameters (e.g. dislocation densities).

** Now: Research Institute for Non-ferrous Metals Freiberg GmbH, D-09599 Freiberg, Germany*

EXPERIMENTAL PROCEDURES / ANALYSIS OF X-RAY DIFFRACTION LINE-BROADENING

The sample material of the present work was polycrystalline zirconium with a purity 99,8+ % and a mean grain size of 11 µm. Using a commercial testing system MTS 810, cylindrical samples of 8 mm diameter and 12 mm height were compressed at RT ($T/T_m = 0.14$) with a strain rate $\dot{\varepsilon} = 10^{-3}\ s^{-1}$ until selected logarithmic strains $\varepsilon \le 1.2$.
The microstructure of the compressed specimens was investigated by means of light microscopy, X-ray diffractometry (line-broadening and texture analysis), and in some cases also by SEM (EBSP – technique). The X-ray substructure analysis was essentially based on the line shapes of the radial intensity distributions of the reflections (10.0), (00.2) and (11.0), which were measured with Co-Kα radiation perpendicular to the stress axis of the compression tests, using a conventional powder diffractometer HZG 4 equipped with a secondary-beam graphite monochromator.
In order to characterise the dislocation content of the specimens, the Stokes-corrected Fourier cosine coefficients A(L) of the individual reflection profiles (L = md(h) - measuring length representing the distance of pairs of lattice cells perpendicular to the scattering lattice planes h = {hkl} with m – Fourier order and d(h) – lattice spacing) were evaluated by means of Krivoglaz - Wilkens plots [5]

$$\Psi(\ln L) = -\ln \frac{A(L)}{L^2} = \frac{1}{LD(h)} + \frac{\pi}{2} h^2 < b^2\chi(h)> \rho \ln \frac{L_0}{L} \tag{1}$$

They allow the estimation of the mean total dislocation density ρ from the slope $-(d\Psi/d\ln L) \sim \rho$ and the distance $L_0 = \eta R_c$ proportional to the outer cut-off radius R of the strain field of the dislocations from the intersection $\Psi(\ln L) = 0$ of a linear branch occurring at large values of L with the abscissa. In the formulas $h = 2\sin\vartheta/\lambda$ is the module of the diffraction vector, b the module of the Burgers vector of the dislocations and $<b^2\chi(h)>$ an averaged orientation factor, which depends on the orientation of the operating diffraction vector with respect to the direction of the Burgers and the line vectors of a special type of dislocations. Because in hexagonal materials a-, c- and (c+a)- dislocations with different Burgers vectors 1/3<11.0>, <00.1> and 1/3<11.3> can be present, the average

$$< b^2\chi(h) >= \sum_i c_i b_i^2 < \chi_i(h) > \tag{2}$$

is the weighted sum (c_i – fractions of the a-, c- and (a+c)-dislocations) of the orientation factors of all existing dislocation families, which additionally must be averaged with respect to the dislocation character and the operating slip systems [6].
Equation (1) shows that the slope

$$B(h) = (\pi/2)\, h^2 < b^2\chi(h)> \rho \tag{3}$$

of the Krivoglaz-Wilkens plot is a linear function of $h^2 = 4\sin^2\vartheta/\lambda^2$. Therefore, taking into account the influence of the elastic anisotropy on the orientation factors $\chi(h)$, the fractions c_i of the dislocations can be obtained by optimal fitting the plot $B(h)/<b^2\chi(h)>$ *vs.* h^2 by a straight line [4]. A similar procedure is possible for the modified Williamson - Hall plot $\beta(h)/\sqrt{<b^2\chi(h)>}$ *vs.* h of the physical line widths $\beta(h)$ of the X-ray reflections [6].

RESULTS AND DISCUSSION

Flow curves at $\dot{\varepsilon} = 10^{-3}\ s^{-1}$ and work-hardening rate

A flow curve $\sigma = \sigma(\varepsilon)$ measured at RT is presented in Fig. 1a. It consists of a nearly linear initial branch and a final parabolic part. According to [7], such a deformation behaviour is typical for the occurrence of both mechanical twinning and dislocation slip.

The Kocks – Mecking plot $\Theta = d\sigma/d\varepsilon = \Theta(\sigma)$ of the flow curve is shown in Fig. 1b. It illustrates that the work - hardening rate $\Theta = d\sigma/d\varepsilon$ is practically constant at strains $\varepsilon < 0.3$ and decreases linearly at stresses above 850 MPa, where the parabolic part of the flow curve be-gins. That means:

- The branch θ = constant of the Kocks – Mecking plot has to be interpreted in terms of both dislocation accumulation (stage II of single – crystal deformation) and mechanical twinning, whereas
- the subsequent decrease of the work – hardening rate indicates stage III behaviour due to cross slip of screw dislocations [8].

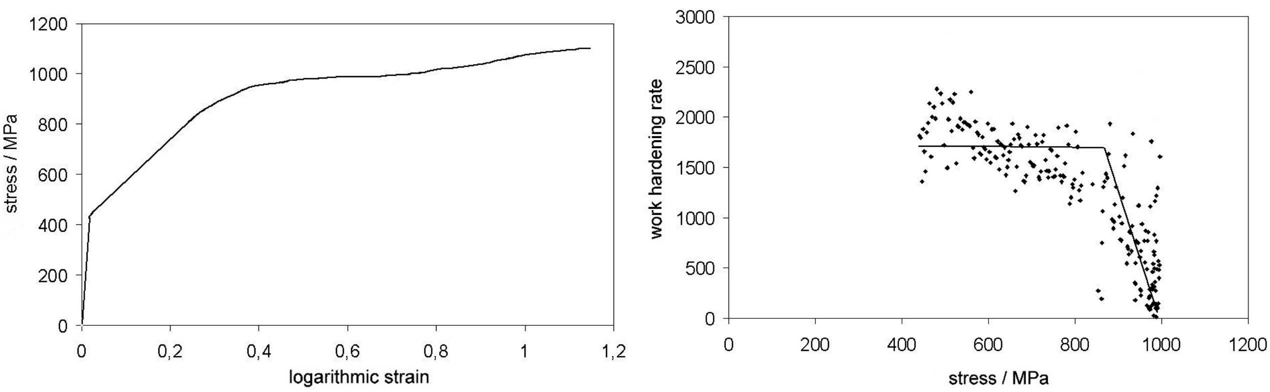

Fig. 1: Flow curve (a) and Kocks – Mecking plot (b) of zirconium compressed at RT.

The material is highly ductile. Up to strains $\varepsilon = 1.2$ no cracks were observed. According to [9] this is also an indication that mechanical twinning contributes essentially to the deformation and that several twinning systems operate.

Mechanical Twinning

Mechanical twinning, which is favoured by the initial texture of the sample material, plays an important role especially in the first stage of deformation. The mean twin size and the (apparent) volume fraction of the twins were estimated using light microscopy. While the mean twin area decreases slightly with increasing strain (Fig. 2a), a maximum of the volume fraction of the twins is observed at low strains in the range $0.15 < \varepsilon < 0.3$. Subsequently, the volume fraction of the twins apparently decreases and remains nearly constant within the range $0.35 < \varepsilon < 0.7$. At higher strains it increases once more (Fig. 2b).

Like in the case of compressed magnesium [2] the apparent decrease of the twinned volume in the range $0.3 < \varepsilon \leq 0.4$ can be explained by multiple twinning, which often occurs in zirconium and reduces the size of the twins ([10], for instance). Twin lamellas with a width $\ell < 1$ µm become invisible in optical micrographs.

The interrelations between the operating twin systems of materials like zirconium ($c/a < \sqrt{3}$) on the crystal orientation are illustrated in Fig. 3. The main twinning system is {10.2}<10.1> and becomes activated in compression in the case of crystallite orientations situated at the margin of the of the standard orientation triangle, which are characteristic for the initial texture of the investigated material (see below). Moreover, twins of the system {11.1}<10.1> due to orientations of the central part of triangle can be expected, while twins of the systems

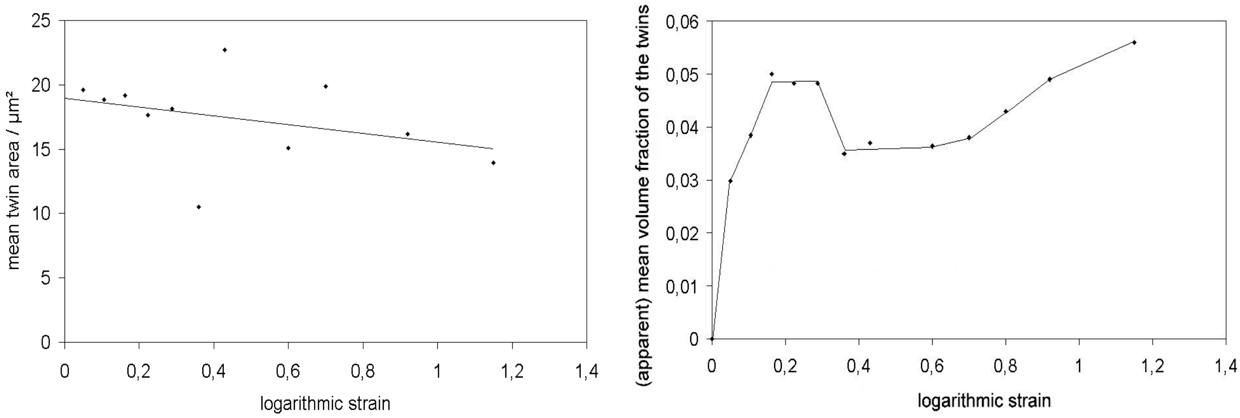

{11.2}<10.1> are very fine and mostly observed in the interior of the coarse primary twin lamellas [11].

a) b)

Fig.2. Mean twin size (a) and apparent volume fraction of the twins (b) in compressed zirconium as estimated by light microscopy.

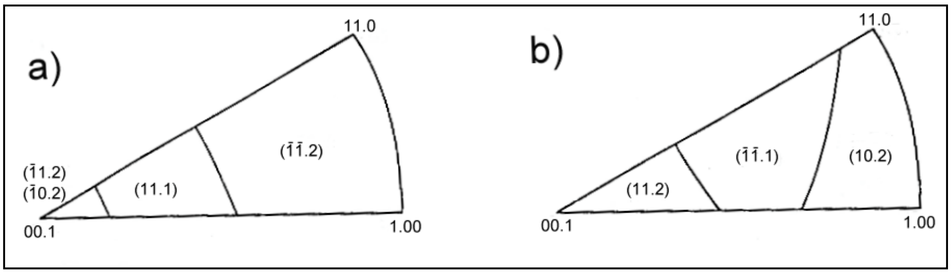

Fig.3. Orientation dependence of mechanical twinning in hexagonal metals for c/a < √3 [12]: (a) tension, (b) compression.

Taking into consideration the lattice rotations and orientation changes accompanying the different twinning operations, the following twin sequence can be assumed:

- Primary twinning on the systems {10.2}<10.1> gives rise to a lattice rotation of 94.87° and changes the crystallite orientation from the margin (initial texture) to the vicinity of the basis pole of the orientation triangle.
- In the basis-orientated crystallites {11.2}<11.3> twinning is activated, which causes a back-rotation of 64.22° into the region of the margin orientations and reduces the size (and the apparent volume fraction) of the microscopically visible twins.
- Because the twins obtained by the secondary process have orientations near the initial texture, they can twin once more through activation of the system {10.2}<10.1>, which leads to the observed re-increase of the volume fraction of the twins (Fig. 2b).

The proposed twin sequence is directly confirmed by EBSD measurements of the lattice misorientations occurring in the compression testes and becomes also visible in the evolution of the compression texture.

Texture development

In the sample material an initial fibre texture with the components {10.0} and {11.0} was observed, where the intensity of the {11.0} component was stronger than that of the {10.0} component. During the compression several strong texture changes occur (Fig. 4), which are primarily the result of twinning processes. Texture changes due to slip are much less intensive [13].

During the first stage of the deformation the pole density of the {10.0} component decreases rapidly with increasing strain and at strains ε ≥ 0.1 it disappears completely. Simultaneously a {00.1} - fibre texture is formed, whose intensity increases slightly up to ε ≈ 0.3. Similarly an increase of the pole density of the component {11.0} is observed.

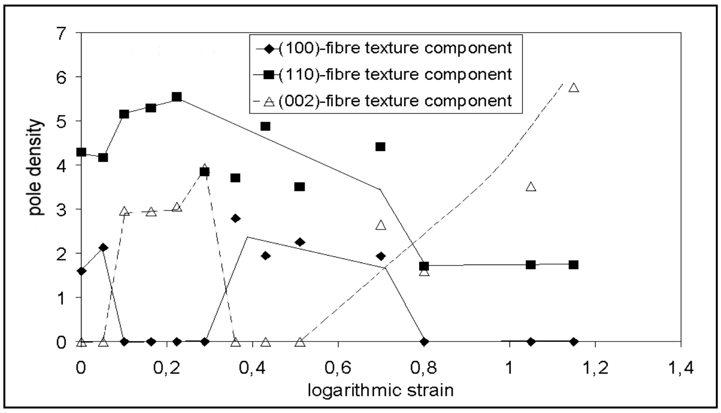

Fig. 4. Pole densities of the texture components versus strain.

The texture transformation is the result of {10.2}<10.1> twinning. According to Fig. 5, all 6 twinning poles can operate in compression. This explains the significant increase of the twinned volume of the specimen at small strains and the rapid formation of the {00.1} fibre texture (Fig. 4).

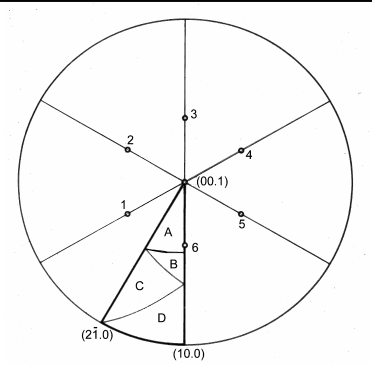

A	1 - 6 in tension
B	2,3,5,6 in tension, 1,4 in compression
C	3,6 in tension, 1,2,4,5 in compression
D	1 - 6 in compression

Fig. 5. Activation of the twinning systems {10.2}<10.1> in hexagonal metals with ratios c/a<√3 [7].

The main slip system of zirconium at RT is the prismatic one. Its activation is restricted in the crystallites of the initial texture components, but possible and should be responsible for the weak increase of the pole density of the {11.0} component in the strain range 0 ≤ ε ≤ 0.3 [14]. However, because the activation of mechanical twinning is easier and the dominating deformation mode.

At strains above ε = 0.3, where the decrease of the apparent volume fraction of the twins is observed, a new {10.0} fibre texture occurs and the {00.1} component disappears. This corresponds to the occurrence of secondary twinning on the systems {11.2}<10.1> discussed above. Further compression leads to repeated twinning on {10.2}<11.0>, which reduces the intensity of the {10.0} component once more and gives rise to the restoration of the {00.1} fibre. At strains ε > 0.6 the component {10.0} disappears again, while, corresponding to the increase of the apparent volume of the twins, the intensity of the {00.1} fibre texture grows.

At strains ε > 0.3 the intensity of the texture component {11.0} decreases, too. As confirmed by EBSD, this is also the result of the {10.2}<11.0> - twinning, which takes place permanently during the whole compression test and dominates the increase of the {11.0} orientations due to prismatic slip. However, the influence of the twinning processes on the texture component {11.0} is much less strong than in the case of the {10.0} fibre.

Evolution of the dislocation density during compression

A fitting procedure of the modified Williamson – Hall plot $\beta(h)/\sqrt{<b^2\chi(h)>}$ *vs*. h determined from the integrated line widths of the reflections (10.0), (00.2), (10.1), (10.2) and (11.0) indicates, that in compression of zirconium texture – related crystallite fractions with significantly different substructures must be distinguished. This agrees with former results obtained with compressed titanium [3,4] but is in some contrast to recent investigations of compressed magnesium polycrystals [1,2], which could well be characterised by a mean dislocation density $\overline{\rho}$.

In the present case a physically realistic value of $\overline{\rho}$ could only be determined for the initial state of the specimens. After deformation the interpretation of the line broadening must carefully take into account the texture development and the dislocation densities of the texture components {10.0}, {00.1} and {11.0.} must be determined separately [5].

Because the compression texture consists of complete fibre components, the separation of the dislocation densities is possible in a simple manner by measuring the corresponding diffraction peaks at the frontal face of the cylindrical specimens. Fig. 6a, b shows the dependence of the physical line width $\beta(h)$ of the X-ray reflections and of the factors B(h) obtained from the Krivoglaz – Wilkens plots of the Fourier coefficients on the strain.

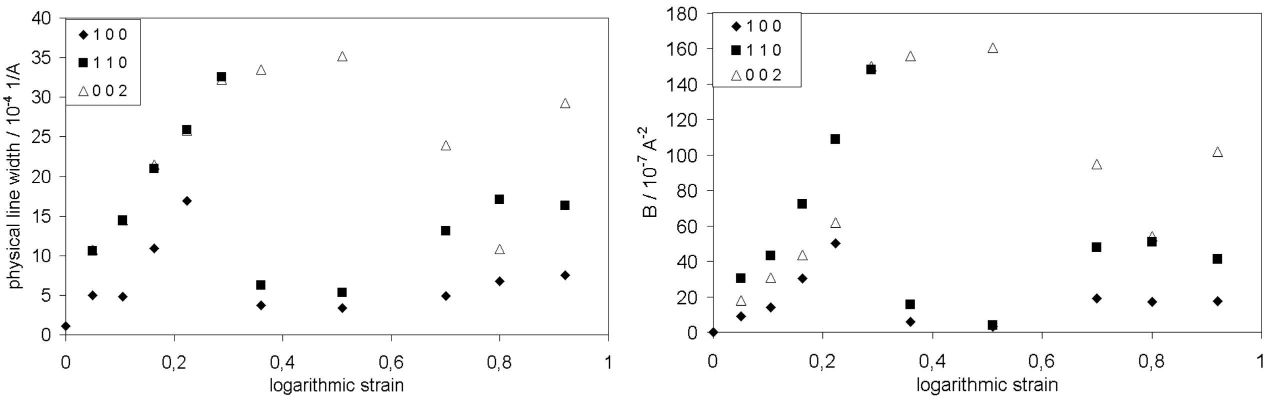

a) b)

Fig. 6. Physical diffraction – peak broadening versus strain: (a) Integrated line widths $\beta(h)$, (b) Factors B(h) from the Krivoglaz - Wilkens plot.

Analogously to the texture development, three regions of different line - broadening can be distinguished:

- increasing of the line widths of all reflections up to strains $\varepsilon \approx 0.3$,
- a drastic reduction of the broadening of the reflections {10.0} and {11.0} within the region $0.3 < \varepsilon < 0.6$, and
- re-increase of the line broadening of the reflection {10.0} and {11.0}, which is accompanied by a significant reduction of the line widths of the reflection {00.2}.

Because processes as recovery or recrystallisation, which would cause a decrease of the dislocation density, are less important or can be excluded at RT ($T/T_m = 0.14$), the drops of the peak broadening of the reflections {10.0} and {11.0} at $\varepsilon \approx 0.35$ and {00.2}at $\varepsilon \approx 0.7$ can only explained with a change of the operating slip systems.

TEM investigations have shown, that in zirconium the prismatic system is the main slip system. Basal slip occurs only at elevated temperatures and/or in the case of unfavourable grain orientation [15]. Another possible slip system is the pyramidal system of the first order [16]. Slip on pyramidal planes of the second order does not occur. The dislocation content consists of a- and a small fraction of (a+c) – dislocations [6], and the a - dislocations have mainly the character of screws [17].

Taking into account these results, the calculations of the orientation factors $\langle b^2\chi(h)\rangle$ needed for the estimation of the dislocation density ρ from the line width $\beta(h)$ or the slope B(h) of the Krivoglaz - Wilkens plot (equation 3) was based on the following assumptions:

- Due to the very small Schmid factors in the texture component {00.1} only pyramidal slip can be activated.
- A fraction of c - dislocations is, if existing, negligibly small. Accordingly, only a- and (c+a) - dislocations are taken into consideration [18].
- In the texture components {10.0} and {11.0} prismatic slip is dominating in the strain range $0 \le \varepsilon \le 0.3$. At higher strains pyramidal slip has to be considered in a greater extent.
- All a - dislocations are screws.

Because the orientation factors $\chi(h)$ for pyramidal slip systems are considerable higher than those for prismatic or basal slip, the changes of the line broadening can now easily be understood and both the magnitude and the strain – dependence of the dislocation densities ρ_h related to the texture components are physically realistic. The densities ρ_h are also in good agreement with values given in the literature [6, 19], but the defect content of the crystallites with the prismatic orientations {10.0} and {11.0} is considerable higher than that of the crystallites with the orientation {00.1}(Fig.7).

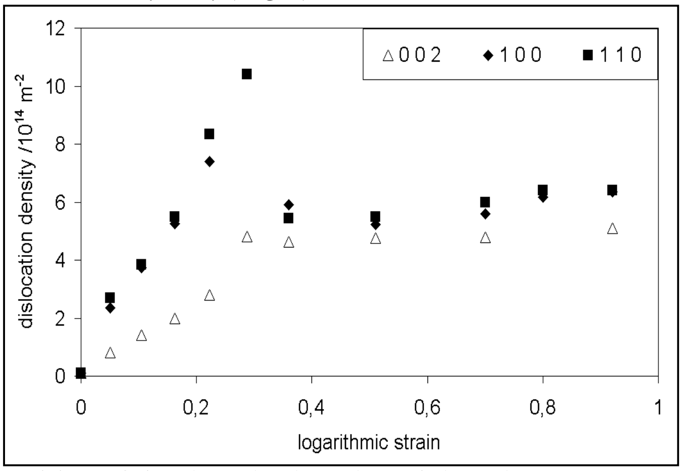

Fig. 7. Dislocation densities of the {10.0}, {11.0} and {00.1} components versus strain.

If the X – ray diffractometry is combined with TEM studies concerning the specification of the character and the fractions of dislocations with different Burgers vectors, further improvement of both the methodology of the substructure analysis and the accuracy of the absolute values of the dislocation densities ρ_h can be expected.

SUMMARY

Microstructure changes occurring in compression tests of zirconium at RT indicate strong interrelations between mechanical twinning, dislocation slip and texture development. The experimental results can be summarised as follows:

- Twinning is identified as an important deformation mechanism. The activation of several twin systems leads to multiple twinning and gives rise to high ductility of the material.
- The sequence of different twinning operations is clearly reflected in the texture development and causes three strain regions, in which the intensities of the observed texture components {10.0}, {00.1} and {11.0} are changed in characteristic manner.

- Analysis of the peak broadening of the X-ray reflections {10.0}, {00.1}, and {11.0} indicates that, due to the operation of different slip and twinning systems, the texture evolution is accompanied by the formation of crystallite fractions with significantly different substructure.
- The interrelation between the texture and the defect content can be clarified by analysis of the line broadening of the reflections {10.0}, {00.1}, and {11.0} measured at the frontal face of the compressed specimens. Of course, the physically realistic interpretation of the results requires a careful consideration of the slip and twinning systems being active in the crystallites of the different texture components.

The present papers demonstrates that the methodology of integrated substructure analysis by X - ray diffractometry is now elaborated sufficiently for a detailed investigation of complex microstructures as occurring in plastically deformed hexagonal metals and alloys. Moreover it is shown once more that substructure analysis in real polycrystalline materials must be related in every case to the evolution of both the global and the local sample texture.

ACKNOWLEDGEMENT

It is gratefully acknowledged that the present work was financially supported by the DFG.

REFERENCES

[1] Pötzsch A. and Klimanek P.: In: Proc. EUROMAT 99 Munich/Germany, Vol.4 Microstructural Investigation and Analysis, Wiley-VCH, Oberursel, 2000, pp. 259-264.
[2] Klimanek P. and Pötzsch A. : In: Proc. IPSMA 8 Prague/Czech Republic, 2000, submitted to Mater. Sci. Eng.
[3] Weidner A. and Klimanek P.: Mat. Sci. Eng. A234-236 (1997) 814.
[4] Weidner A.: Dr. - Ing. Thesis. Freiberger Forschungsheft B300, 1999.
[5] Klimanek P.: In: X-ray and Neutron Structure Analysis in Material Sciences, J.Hasek (Ed.). Plenum Press, New York, 1989, pp. 125-137.
[6] Kuzel jr. R. and Klimanek, P.: J. Appl. Cryst. 21a, (1988) 59; J. Appl. Cryst. 21b, (1988) 363; J.Appl. Cryst. 22, (1989) 299.
[7] Hötzsch G.: Habilitation Thesis, Freiberg Academy of Mining, Germany, 1970.
[8] Mecking H. and Kocks U. F.: Acta metall. 29, (1981) 1865.
[9] Yoo M. H.: Metall. Trans. A 12 (1981) 409.
[10] Tenckhoff E.: Metall. Trans. A 9 (1978) 1401.
[11] Lin X., Huifang, G. and Haicheng, G.: In: Proc. ISCMA 10, Sendat/Japan 1994 - The Japan Institut of Metals, 1994, pp. 163 - 166.
[12] Munroe N. and Tan X. : Sc. Mat. Vol. 36 (1997) 1383.
[13] Salinas Rodriguez A. and Jonas J.J.: Met. Trans. A Vol.23a (1992) 271.
[14] MacEwen S. R., Christodoulou N., Tome C., Jackman J. and Holden T. M.: In: Proc. ICOTOM 8, (Eds. J. S. Callend and G. Gottstein). The Metallurgical Society, 1988, pp. 825-836.
[15] Akhtar A.: Acta Met. 21 (1973) 1.
[16] Francillette H., Bacroix B., Gasperini M. and Bechade, J. L.: Mater. Sci. Eng. A 234 – 236 (1997) 974.
[17] Kohn E. and Dunne D. P.: Metallography 10 (1977) 371.
[18] Miyada - Naborikawa L. T., de Batisi R. and Delavignette, P.: Phys. Stat. Sol. A 89, (1985) 521.
[19] Trojanová Z., Smola B., Lukáš P. and Dlouhý, A.: In: Proc. ICSMA 7, Montreal, 1985, pp. 171 - 176.